Needs for Flexibility Caused by the Variability and Uncertainty in Wind and Solar Generation in 2020, 2030 and 2050 Scenarios

Koivisto, Matti Juhani; Sørensen, Poul Ejnar; Maule, Petr; Nuño Martinez, Edgar

Publication date:
2017

Document Version
Publisher's PDF, also known as Version of record

Needs for Flexibility Caused by the Variability and Uncertainty in Wind and Solar Generation in 2020, 2030 and 2050 Scenarios

Matti Koivisto, Poul Sørensen, Petr Maule, Edgar Nuño
DTU Wind Energy

***Abstract*— The growing share of variable renewable energy sources (VRE) in Nordic and Baltic countries is expected to increase the need for flexibility in the energy systems. VRE generation is highly variable because it is determined by weather conditions, and it is uncertain due to forecasting errors. Both of these aspects will be considered for the analysed 2020, 2030 and 2050 scenarios. In addition to the variability in VRE generation, the variability in net load (electricity consumption subtracted by the VRE generation) is analysed. The results show that, compared to hourly ramp rates in consumption, the hourly ramp rates of the net load are not expected to increase significantly; however, there is a modest increase in 2050. The relative variability of the net load is expected to increase significantly when going from 2014 to 2050. Wind generation forecasting uncertainties are assessed for 5 minute, 15 minute and hour ahead forecasts. It is shown that the forecasting error probability distributions are fat-tailed, which means that the risk of experiencing a large forecasting error is higher than what one would expect assuming normality.**

***Keywords*— forecast errors, ramp rates, solar power, variable generation, wind power**

1. INTRODUCTION

This paper looks at the additional needs for flexibility caused by the growing share of variable renewable energy sources (VRE) in Nordic and Baltic countries. VRE generation is highly variable because it is determined by weather conditions, and it is uncertain due to forecasting errors. Both of these aspects are considered in this report. The VRE generation variability and uncertainty are analysed using installed capacities for scenarios 2020, 2030 and 2050, and also for 2014. The scenarios are the baseline scenarios from [1], and they are used as the baseline scenarios in the Flex4RES project. Further discussion on the scenarios is given in Section 8.10.

In addition to analysing the variability in VRE generation, this paper also examines the variability in net load (electricity consumption subtracted by the VRE generation). Analysis of the net load is important, as it is the load that has to be served by other generation types (such as hydro power). Alternatively, the variability in the net load can be managed by demand-side response, transmission of power to or from surrounding countries or by storing energy.

The geographical distribution of the installed VRE generation affects the probability distribution (PD) of the aggregate generation, including the probabilities of very low or high generation. It has been shown that geographically concentrated installed wind generation yields high probabilities for very high or low aggregate generation, while geographically dispersed installations provide aggregate generation with less variability [2], [3]. For solar generation, the effect of the geographical distribution is less significant [4]. A combined modelling of wind and solar power has been presented, for example, in [5]. This paper provides a combined analysis of wind and solar power applied to multiple Nordic and Baltic countries, and shows how the variability of the aggregate VRE generation behaves when both generation types are present in the generation mix.

The first need for flexibility analysed in this report is the one caused by the variability in VRE generation (even if the generation could be forecasted perfectly). The need is analysed in relation to the net load, considering both the variability of the net load and the expected ramp rates in the different scenarios. The second analysed need for flexibility looks at the 5 minute, 15 minute and one hour ahead forecasting errors in wind generation (the utilized methodology does not currently support solar generation forecasting error modelling; however, this capability will be implemented in the future, as discussed in Section 8.4). There are other significant effects a high share of installed VRE generation can have on the power system, such as the possible challenges caused by low inertia when the share of VRE generation is high [6]. However, these issues are not considered in this paper.

The paper is structured as follows. Section 2 introduces the scenarios analysed in this paper. It also presents the methodology used for simulating the wind and solar generation time series, and forecast errors for wind generation. Section 3 describes the important effects the geographical distribution of installed VRE generation has on the variability of the aggregate generation, and describes the important statistical properties of wind and solar generation time series.

Considering the needs of the Flex4RES project, hourly resolution is used for assessing the variability in the VRE generation in Section 4 and in the net load in Section 5 (this corresponds to the hourly working Nordpool market [7]). The uncertainties in wind generation forecasting are analysed on a 5 minute resolution in Section 6. Based on the results from Sections 5 and 6, Section 7 describes the additional needs for flexibility in the different scenarios. Section 8 provides further discussion on some of

the most important aspects of the presented methodology and information on the planned updates to the presented VRE simulation methodology. Section 9 concludes the paper.

2. Wind and Solar Generation Simulations

This section presents the installed VRE generation capacities in the analysed scenarios. In addition, the methodology used for simulating the hourly VRE generation time series is presented. The methodology is also used to provide 5 minute, 15 minute and hour ahead wind generation forecasts.

2.1. Installed VRE Generation Capacities in the Scenarios

The analysed Nordic and Baltic areas are shown on a map in Fig. 1. The installed VRE generation capacities in the individual areas for the different scenarios, which are the baseline scenarios from [1], are presented in Appendix A. Further discussion on the scenarios is given in Section 8.10. Table I shows the installed capacities of the different VRE types aggregated to the whole analysed region. It can be seen that the relative share of installed offshore wind generation capacity first increases when going from 2014 to 2020, but then decreases all the way to 2050 (in between 2030 and 2050 there is expected to be no net offshore installations in any analysed country, as seen in Appendix A). The relative share of installed solar generation capacity decreases all the way from 2014 to 2050, with almost no change in net solar generation capacity between 2030 and 2050. Thus, onshore wind generation is the dominant source of VRE generation in all scenarios, with its relative share rising to 91% in 2050.

Table II shows how the installed onshore wind generation capacity in the scenarios is divided to different regions in the analysed scenarios. Going from 2014 to 2020, the geographical distribution moves away from Denmark and southern Sweden (SE3 and SE4), i.e., away from the region with currently high installed wind generation capacity, towards a more dispersed overall geographical distribution. Going from 2020 to 2030, the proportional share in Denmark decreases, however, the share in Southern Sweden stays almost the same, and the share in Finland (which is relatively far away from Denmark and southern Sweden) decreases. The share in the Baltic countries increases significantly, and the end result is a slightly increased geographical spread for 2030. The relative shares in 2050 are quite similar to 2030; however, the share in southern Sweden increases a little. Section 3 shows the effects the changing geographical distribution can have on the aggregate VRE generation.

Fig. 1. Map with the Nordic and Baltic areas included in the analyses (they are the Nordpool bidding areas [7], except for Finland that is divided into two areas).

TABLE I. Installed VRE generation capacities in the Scenarios

Scenario	Offshore wind (GW)	Onshore wind (GW)	Solar (GW)	Total (GW)
2014	1.46 (12%)	9.78 (82%)	0.65 (5.4%)	11.9
2020	3.56 (17%)	15.9 (78%)	0.99 (4.9%)	20.4
2030	3.87 (11%)	30.6 (84%)	1.76 (4.9%)	36.3
2050	3.87 (6.4%)	54.3 (91%)	1.75 (2.9%)	60.0

Aggregate VRE generation capacities for the Nordic and Baltic areas included in the analyses (the percentages in the brackets show the shares of the different VRE types compared to the total). The installed capacities for the individual areas are shown in Appendix A.

TABLE II. SHARES OF THE INSTALLED ONSHORE WIND CAPACITIES IN DIFFERENT REGIONS IN THE SCENARIOS

Scenario	DK	SE south (SE3 and 4)	NO south (NO1, 2 and 5)	SE north (SE1 and 2)	NO north (NO3 and 4)	Baltic countries	FI
2014	36%	29%	3%	15%	6%	7%	4%
2020	26%	18%	3%	15%	20%	9%	10%
2030	17%	18%	5%	19%	18%	17%	5%
2050	15%	22%	3%	20%	19%	18%	3%

Aggregate installed onshore wind generation capacities in the different regions as percentages of the aggregate onshore wind capacity shown in Table I. The installed capacities for the individual areas are shown in Appendix A.

2.2. CorWind

CorWind is a tool developed at DTU Wind Energy for simulating wind power generation time series. As this paper focuses on the simulation results and their effects on the needs for flexibility, only a very short overview of CorWind and its capabilities is given here. An overview of the CorWind simulation work flow is shown in Fig. 2. CorWind is based on a meteorological database, which is in hourly resolution. Mesoscale weather models, such as the WRF model, generally underestimate the variability of wind speeds [8]. Thus, CorWind adds fluctuations to the WRF wind speeds in order to provide simulated wind speed time series with more realistic variability. This also allows CorWind to simulate data with higher than hourly resolution.

When representing a wind farm in CorWind, an aggregate power curve is used. Based on the simulations of individual wind farms, an area-wise aggregated power curve was estimated for each onshore area. The area-wise aggregated power curves are used with weighted mean wind speeds (weighted by the wind generation capacities of the individual wind farms within each area). For offshore wind generation, each wind farm was simulated separately, and the resulting time series were aggregated to reach the aggregate wind generation time series for each offshore area.

As described in the previous subsection, each scenario specifies the installed onshore and offshore wind generation capacities for each analysed area. Five meteorological years (2011 to 2015) were used to simulate five years of wind generation time series for each scenario (i.e., the simulated time series for the 2020 scenario describe what would have been generated between 2011 and 2015 if the installed capacities would have been as they are in the 2020 scenario).

In addition to the simulated hourly wind generation time series (used in Sections 3-5), CorWind is used to simulate 5 minute, 15 minute and hour ahead wind generation forecasts (used in Section 6). These simulations model the error inherent in wind speed forecasts that are based on meteorological models. The use of these simulated meteorological wind generation forecasts in estimating short term uncertainties in wind generation forecasting is presented in Section 6.1.

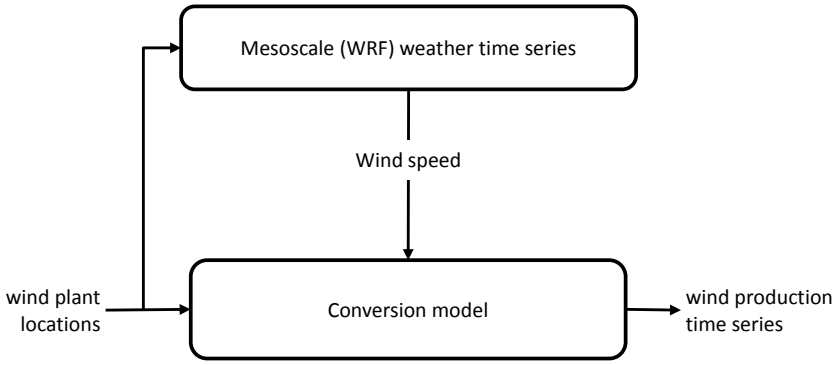

Fig. 2. An Overview of the CorWind simulation work flow. In addition to wind generation time series, CorWind also provides simulated wind forecast time series.

2.3. Solar Generation Simulations

The solar generation simulation model is based on the same meteorological database as CorWind. This gives the appropriate dependencies between the irradiance and wind speed time series, and thereby between the solar and wind generation time series. An overview of the solar generation simulation work flow is shown in Fig. 3. It was assumed that the panels face south and the tilt angles are 35 degrees for all locations. Although ambient temperature and wind speed are possible inputs to the PV plant model, they were not used in the simulations presented in this paper; planned updates to the irradiance to power conversion are presented in Section 8.5.

As with the wind generation simulations, 5 meteorological years (2011 to 2015) were used to simulate five years of solar generation time series for each area for each scenario. The solar generation simulation methodology does not currently support forecast simulations (more discussion is given in Section 8.4).

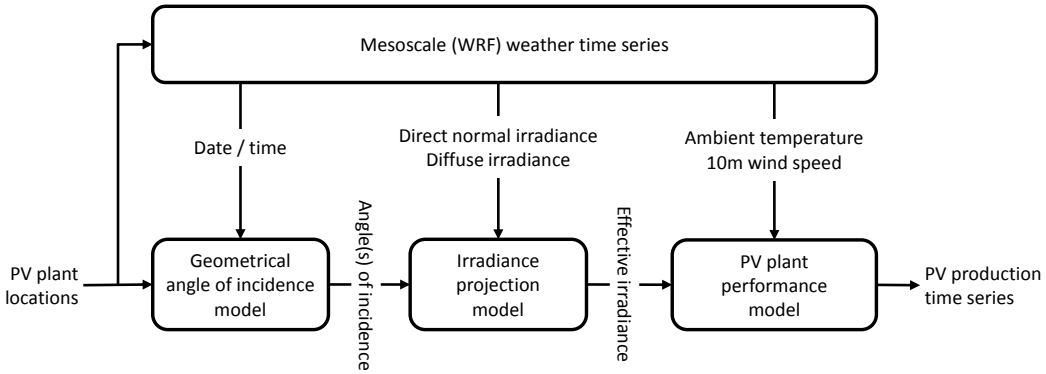

Fig. 3. An overview of the solar generation simulation work flow.

3. Effect of the Geographical Distribution of Installed VRE Generation

This section presents a statistical view on how the variability of the aggregate VRE generation changes when the constituent parts (the individual areas), and the relations between them, have certain statistical properties. It is shown that the correlations between the areas have a significant effect on the PD of the aggregate generation. The analyses are presented for hourly data.

3.1. Relative Standard Deviation of Aggregate VRE Generation

The simulated VRE generation data (generated as presented Sections in 2.2 and 2.3) are proportion of installed capacity (PIC) values [1], i.e., they are always between 0 and 1 (where 1 means generation at the full installed capacity). The data is denoted as $\boldsymbol{y}_t = [y_{1,t},..., y_{k,t}]'$, where $y_{i,t}$ is the PIC generation of i at time t. Index i denoted all VRE types for all analysed areas, e.g., three VRE types for two areas gives $k = 6$. The expected value of the aggregate VRE generation of these multiple VRE generation types in different areas at time t is

$$\mathrm{E}(p_{\mathrm{aggr},t}) = \sum_{i=1}^{k} c_i \mathrm{E}(y_{i,t}), \tag{1}$$

where $\mathrm{E}(y_{i,t})$ is the expected value of the PIC generation of i, and c_i is the installed VRE generation capacity of i. The standard deviation (STD) of the aggregate VRE generation is

$$\mathrm{Std}(p_{\mathrm{aggr},t}) = \sqrt{\sum_{i=1}^{k} c_i^2 \sigma_{i,t}^2 + 2\sum_{i=1}^{k-1}\sum_{j=i+1}^{k} c_i c_j \rho_{i,j;t} \sigma_{i,t}\sigma_{j,t}}, \tag{2}$$

where $\sigma_{i,t}$ is the standard deviation of the PIC generation of i and $\rho_{i,j;t}$ is the (Pearson's) correlation between the generation of i and j [2]. The standard deviation of the aggregate VRE generation thus depends both on the variability of VRE generation at the individual areas, and on the correlations between the different areas (and between the different types of VRE generation).

Equation (2) is the definition of the variance of a sum of correlated random variables (RVs), where each RV is multiplied by c_i. Fig. 4 shows an example of how the relative standard deviation (RSD), i.e., STD divided by the expected value, of the sum changes when multiple RVs, with different correlations between them, are summed up (here $c_i = 1$ for all i). As expected, if the correlations are all 1 (i.e., all RVs get always the same values), the RSD does not change. The lower the correlations between the RVs are, the faster the RSD of the sum decreases.

The same principle shown in Fig. 4 applies to the effect of the geographical distribution of installed VRE generation: lower correlations between the VRE generation at the different areas (and between the different VRE types) implies lower RSD of the aggregate generation. Low RSD of generation is desirable, because it means low variability with high mean generation (with no variability in generation, RSD would be 0).

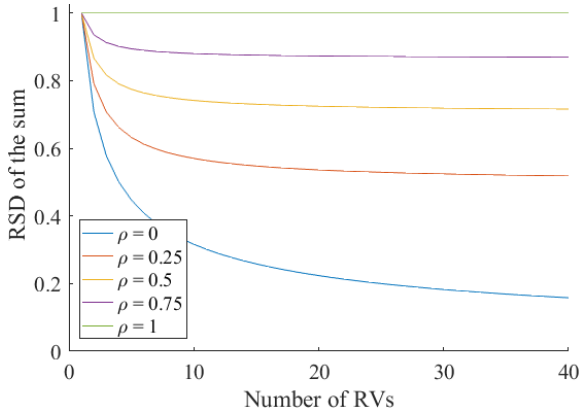

Fig. 4. RSD of the sum of RVs when the individual RVs all have a mean of 1 and STD of 1, and the correlation between each RV is ρ.

3.2. Decrease in Wind Generation Variability as the Aggregated Geographical Area Increases

As the spatial correlations between wind generations in the different areas are lower than 1 for all analysed areas (as can be seen in Appendix B), the RSD of the aggregate generation is expected to decrease when more areas are aggregated (assuming that the mean generations are relatively similar in the different areas). An example of this is shown in Table III. When moving from one Danish area to the whole of Denmark, and then to the whole Nordic and Baltic region, the RSD of the aggregate PIC wind generation decreases. Table III also includes the STDs of the 1st differences of the generation. It can be seen that these values also decrease when more areas are aggregated; however, these changes are discussed more in Section 3.4.

In addition to the first and second moment information in Table III (i.e., mean and STD), Fig. 5 shows the changes in the aggregate PIC wind generation PD as a whole. It can be seen that in addition to the reduction in RSD, the changes in the shape of the PD are also positive: when looking at only area DKw onshore, there are two modes (i.e., the two most likely cases are either full generation or no generation). However, when moving to a higher geographical level of aggregation, the probability mass moves closer to the expected value and the PD moves to a unimodal distribution.

TABLE III. DESCRIPTIVE STATISTICS FOR PIC WIND GENARATION AT DIFFERENT LEVELS OF GEOGRAPHICAL AGGREGATION IN THE 2014 SCENARIO

Aggregated area	Mean	STD	RSD	5th percentile	95th percentile	STD of 1st diff
DKw onshore	0.316	0.277	0.879	0.016	0.895	0.048
All Denmark (also offshore)	0.354	0.272	0.769	0.030	0.885	0.038
All Nordic and Baltic (also offshore)	0.317	0.190	0.601	0.081	0.690	0.021

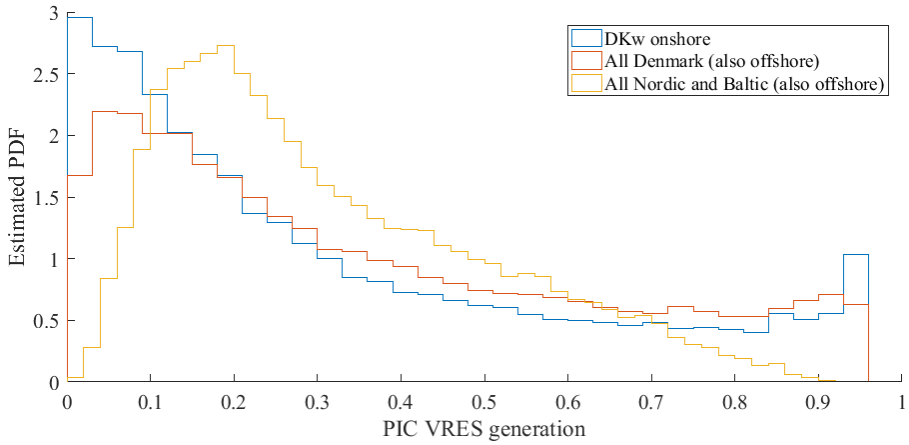

Fig. 5. Estimated PDFs (using histograms) of the hourly PIC wind generation at different levels of geographical aggregation in the 2014 scenario.

3.3. Spatial Correlations between the Different VRE Generation Types

As can be seen in appendix B, the RSD values for solar power are significantly higher than for wind generation. This means that (in the Nordic and Baltic countries, and when looking at a full year on hourly resolution), solar generation has significant variability. However, this variability is somewhat different from the variability in wind generation, as a large part of it is deterministic, i.e., caused by the movements of the sun and the earth [4]. This means that a significant part of the variability should be highly predictable (this is discussed more in Section 8.4). However, even if the variability can be forecasted, the power

system must have enough flexibility to handle it.

Table IV describes spatial correlations between the different VRE generation types (all correlations between all areas are shown in appendix B). It can be seen that the correlations between solar and wind generation are slightly negative between all areas (and within the same areas). As seen in (2), low correlations between the different areas imply low STD of the aggregate generation, and negative correlations imply even lower STD. However, as solar generation has lower mean PIC generation values than wind generation for all areas (as seen in Appendix B), the RSD of the aggregate generation is not necessarily lower when solar generation is added to the VRE generation mix.

As seen in Table IV and appendix B, the spatial correlations between solar generations at different areas are high, and they do not decrease significantly even when the areas are geographically relatively far from each other. This is expected [4], and reflects the correlation caused by deterministic factors, i.e., by the movements of the sun and the earth. However, when considering a relatively large geographical area in the west-east axis, the movement of the sun can also decrease the spatial correlation, as can be seen in Fig. 6. When looking at the northern and southern Finland, the cross-correlation function (XCF) gets its highest value at lag 0; however, when looking at southern Finland and one of the most westerly Norwegian areas, the peak is at lag 2. Thus, the west-east distance between the areas can decrease the spatial correlation.

TABLE IV. AVERAGE SPATIAL CORRELATIONS FOR DIFFERENT VRE GENERATION TYPES

	Offshore wind	**Onshore wind**	**Solar**
Offshore wind	0.40 (0.13... 0.81)	0.38 (0.04... 0.91)	-0.13 (-0.22... -0.05)
Onshore wind		0.33 (0.02... 0.84)	-0.12 (-0.28... -0.03)
Solar			0.89 (0.74... 0.98)

The presented correlations are averages of all the spatial correlations estimated from the simulated data; the values in the brackets are the minimum and maximum correlations of the different area pairs (all correlations are shown in Appendix B).

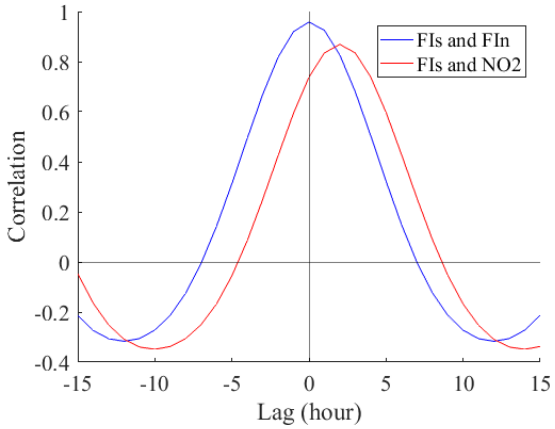

Fig. 6. The estimated XCFs between the simulated solar generation in southern and northern Finland and between southern Finland and one of the most westerly Norwegian areas (NO2). XCF is a discrete function, but it is plotted here as continuous for easier viewing

3.4. Autocorrelation of Hourly VRE Generation

In addition to the PD of the aggregate generation, the geographical distribution of installed VRE generation also affects the temporal dependency structure of the aggregate generation. Fig. 7 shows the average autocorrelation functions (ACFs) for onshore and offshore wind generation, for solar generation, and for the aggregate VRE generation in the 2014 scenario. It can be seen that the aggregate generation has significantly higher ACF values than any of the individual VRE types. The scatter plot behind ACF(1), i.e., the correlation between consecutive hours, for the aggregate VRE generation is presented in Fig. 8.

High ACF(1) value means that there are rarely significant changes from one hour to another (as can be seen in Fig. 8), which implies low relative ramp rates. For hourly data, the one hour ramp rate is the first difference of the data; for example, for the aggregate PIC VRE generation it is $\Delta y_{\mathrm{aggr},t} = y_{\mathrm{aggr},t} - y_{\mathrm{aggr},t-1,}$. The closer to a straight line the points in Fig. 8 are, i.e., the higher the ACF(1) value is, the lower the ramp rates are (because if $y_{\mathrm{aggr},t} = y_{\mathrm{aggr},t-1}$, then $\Delta y_{\mathrm{aggr},t} = 0$). The decrease in the STD of the 1st difference observed in Table III is thus as expected (i.e., a larger geographical level of aggregation implies lower relative ramp rates).

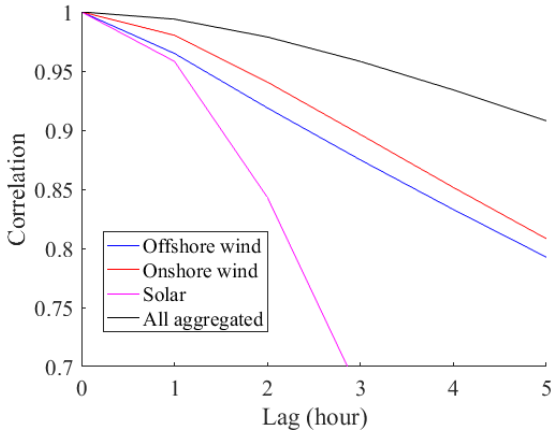

Fig. 7. Average ACFs of the onshore and offshore wind generation and solar generation (averages of the ACFs estimated for all areas), and ACF of the aggregate VRE generation in the 2014 scenario. ACF is a discrete function, but it is plotted here as continuous for easier viewing.

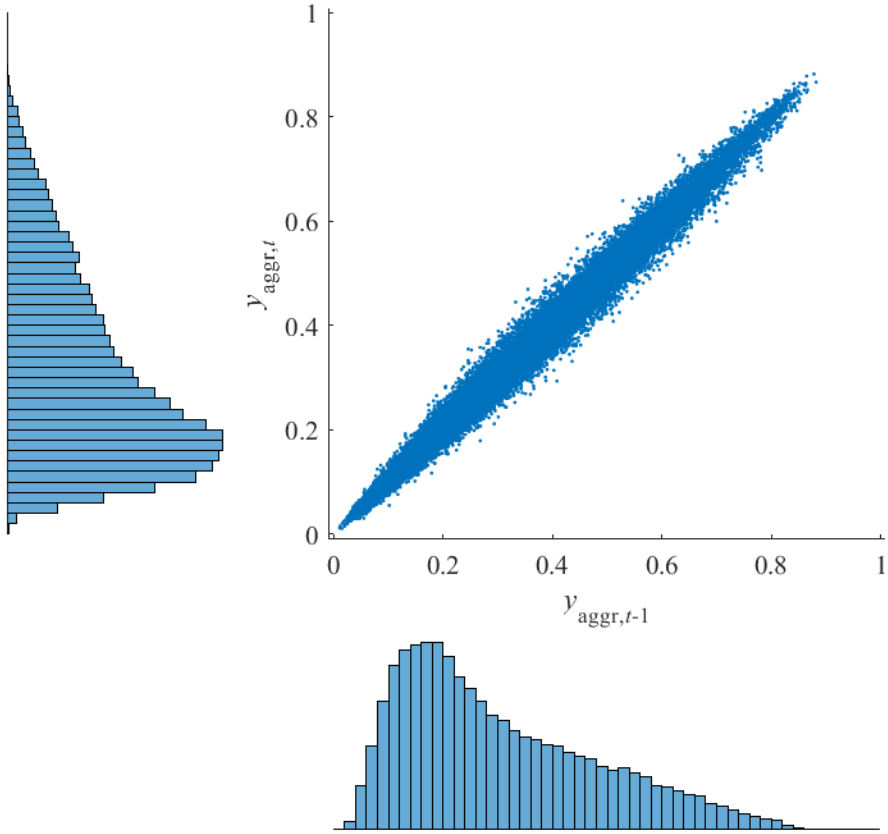

Fig. 8. The scatter plot (with histograms) behind ACF(1) for the simulated aggregate PIC VRE generation for the 2014 scenario (correlation is 0.994).

4. Variability in Hourly VRE Generation in the Different Scenarios

This section presents the estimated variabilities in the aggregate VRE generation in the analysed scenarios. The results are presented four hourly generations and for one-hour ramp rates (i.e., the 1st difference of hourly generation).

4.1. Variability of the Aggregate Generation

The estimated PDFs of the hourly aggregate VRE generation in the different scenarios are presented in Fig. 9, and related descriptive statistic can be seen in Table V. Going from 2014 to 2020, the RSD of the aggregate PIC generation decreases, which is expected considering the increasing dispersion of the overall geographical distribution of installed VRE generation (as was described in Section 2.1). Going from 2020 to 2050, the RSD remains relatively similar. This is expected, as the overall geographical distribution of the installed VRE generation capacity remains relatively similar from 2020 to 2050.

It is important to note that the analyses presented in this report do not include the possible changes in the geographical distributions of installed VRE generation capacity within the analysed areas. These changes can be significant, and can affect the variability of the aggregate VRE generation in the future scenarios, especially in the 2030 and 2050 scenarios. This is discussed

more in Section 8.1.

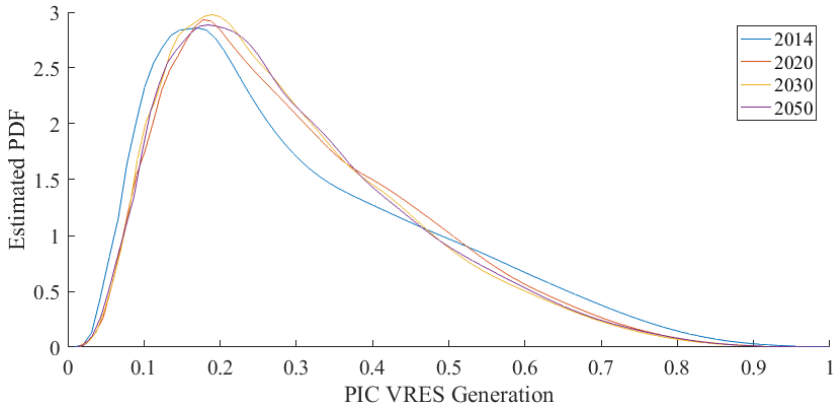

Fig. 9. Estimated PDFs (using kernels) of the aggregate hourly VRE generation in the different scenarios.

TABLE V. DESCRIPTIVE STATISTICS FOR THE AGGREGATE VRE GENERATION

Scenario	Mean	STD	RSD	5th percentile	95th percentile
2014	0.305	0.179	0.586	0.085	0.656
2020	0.305	0.161	0.527	0.096	0.616
2030	0.296	0.156	0.528	0.096	0.602
2050	0.299	0.158	0.530	0.096	0.609

The presented values are for the aggregate hourly PIC VRE generation.

4.2. Ramp Rates of the Aggregate VRE Generation

The estimated PDFs of the 1st differences of the aggregate PIC VRE generation, i.e., $\Delta y_{\mathrm{aggr},t}$, for the different scenarios are shown in Fig. 10, and related descriptive statistics are shown in Table VI. The $\mathrm{RSD}_{\mathrm{diff}}$ is defined as STD of $\Delta y_{\mathrm{aggr},t}$ divided by $\mathrm{E}(y_{\mathrm{aggr},t})$, i.e., it compares the STD of the hourly ramp rate to the mean generation (and thus to the expected yearly generation). It can be seen that the hourly PIC ramp rates are expected to decrease (i.e., the probability mass in Fig. 10 is moving closer to zero) when moving from 2014 to 2020. The ramp rates are expected to decrease slightly from 2020 to 2030, and then increase slightly from 2030 to 2050. The changes in the STD of the PIC ramp rates follow roughly the changes seen in the STD of the hourly generation, as presented in Table V.

As with the results presented in the previous subsection, it is important to note that the analyses presented in this report do not include the possible changes in the geographical distributions of installed VRE generation capacity within the analysed areas. These changes can be significant, and they can change the variability of the aggregate VRE generation in the future scenarios. This is discussed more in Section 8.1.

$\Delta y_{\mathrm{aggr},t}$ is conditional on the value of $y_{\mathrm{aggr},t-1}$, e.g., if $y_{\mathrm{aggr},t-1} = 0$, the change to the next hour must be non-negative. The results presented in Fig. 10 and Table VI thus describe ramp rates on average when looking at the all the hours of the year (however, as very low or high generation values are relatively rare in highly aggregated scenarios, such conditions are relatively rare in the analysed scenarios).

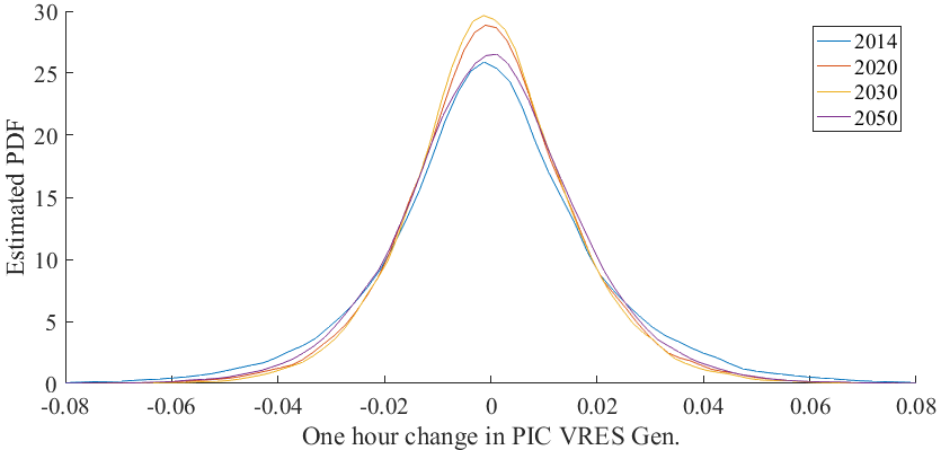

Fig. 10. Estimated PDFs (using kernels) of the 1st difference of the aggregate hourly VRE generation in the different scenarios.

TABLE VI. DESCRIPTIVE STATISTICS FOR THE 1ST DIFFERENCE OF THE AGGREGATE VRE GENERATION IN THE SCENARIOS

Scenario	STD	RSD_{diff}	5th percentile	95th percentile
2014	0.0197	0.0646	-0.0318	0.0332
2020	0.0161	0.0528	-0.0259	0.0267
2030	0.0154	0.0519	-0.0247	0.0256
2050	0.0169	0.0566	-0.0276	0.0279

The presented values are for the aggregate hourly PIC VRE generation. The RSD_{diff} is defined as STD of $\Delta y_{aggr,t}$ divided by $E(y_{aggr,t})$.

5. VARIABILITY IN HOURLY NET LOAD IN THE DIFFERENT SCENARIOS

This section compares the aggregate VRE generation in the different scenarios to the aggregate electricity consumption of the analysed Nordic and Baltic countries. The analysis of the resulting net load is important, as it has to be covered by other generation sources, or managed using other sources of flexibly (e.g., demand-side response).

5.1. The Consumption Time Series

One year of hourly consumption data for 2012, which was acquired from ENTSO-E [9], was used to calculate the net load (by subtracting the simulated VRE generation using the 2012 meteorological year from it). Using more consumption data, and how it can improve the modelling, is discussed in Section 8.6.

The aggregate consumption time series can be seen in Fig. 11, and the scatter plot depicting the one-hour changes in consumption can be seen in Fig. 12. The somewhat distinct upper set of points in Fig. 12 consists of the working day morning hours when there can be a significant up-ramping during one hour. Comparing Fig. 12 to Fig. 8, it can be seen that the correlation between consecutive hours is higher for the aggregate VRE generation than for the aggregate consumption.

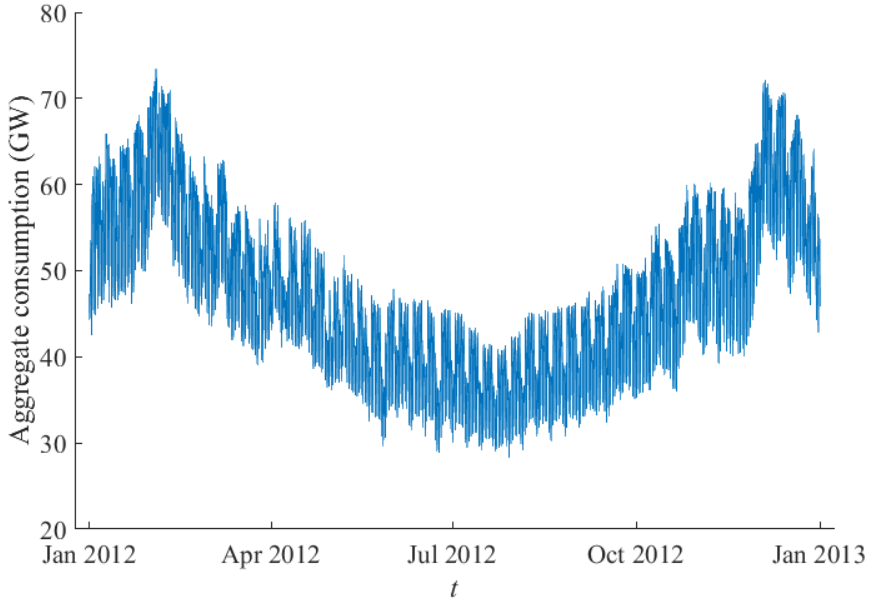

Fig. 11. Aggregate hourly consumption time series of the analysed countries in 2012. Data was acquired from ENTSO-E [9].

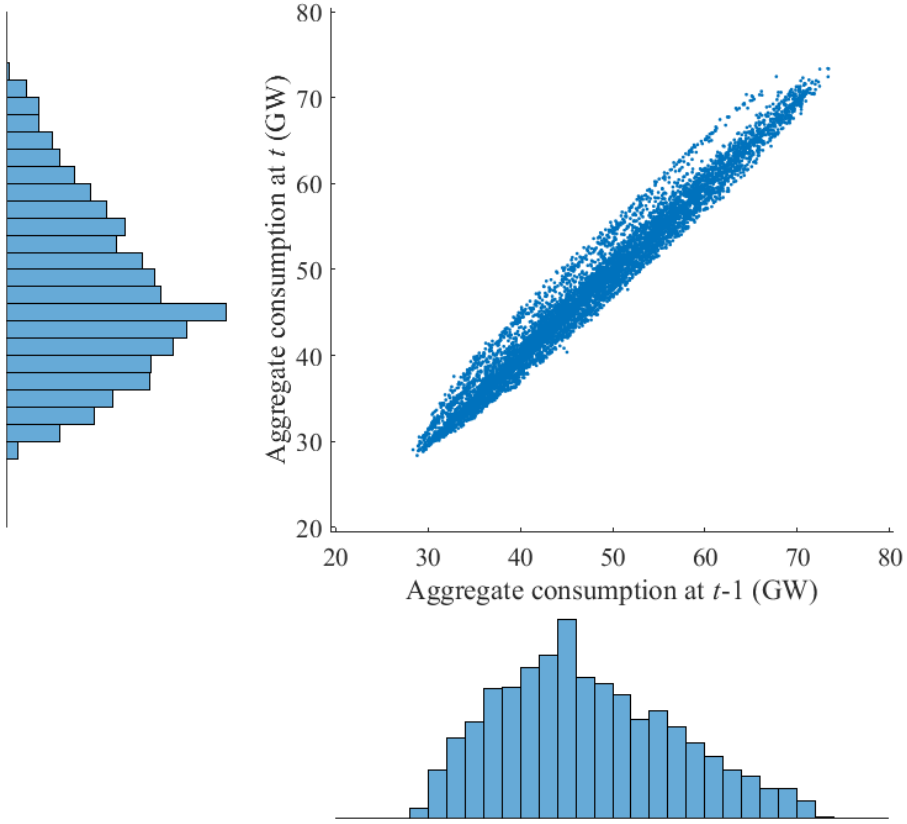

Fig. 12. The scatter plot (with histograms) for the hourly aggregate consumption in 2012 at *t*-1 and at *t* (correlation is 0.986).

5.2. Variability of the Aggregate Net Load

Fig. 13 shows the PDFs of the aggregate net load in the different scenarios (assuming 2012 consumption), and the related descriptive statistics are shown in Table VII. Going from 2014 to 2050, the mean of the net load decreases, because the installed VRE generation generates more and more energy. Somewhat surprisingly, the STD of the net load does not change significantly from 2014 to 2020, and increases only slightly when reaching 2030. However, in 2050 the STD increases modestly. As can be seen in Fig. 13, the probability mass moves closer to zero, and in 2050 there are some hours when the aggregate VRE generation is higher than the aggregate consumption (i.e., net load is negative).

Even though the STD of the net load does not increases very significantly when going from 2014 to 2030, the nature of the variability in VRE generation has a significant consequence on the shapes of the PDs in Fig. 13: there is always some probability

that the aggregate VRE generation is zero (although this probability is very low when the installed VRE generation capacity is highly geographically spread). Thus, the very highest percentiles of the PDs in Fig. 13 must be very similar for all the different VRE generation scenarios; this is phenomena is described in more detail in [10]. However, the estimation of the highest percentiles requires much more data; this is discussed more in Section 8.6.

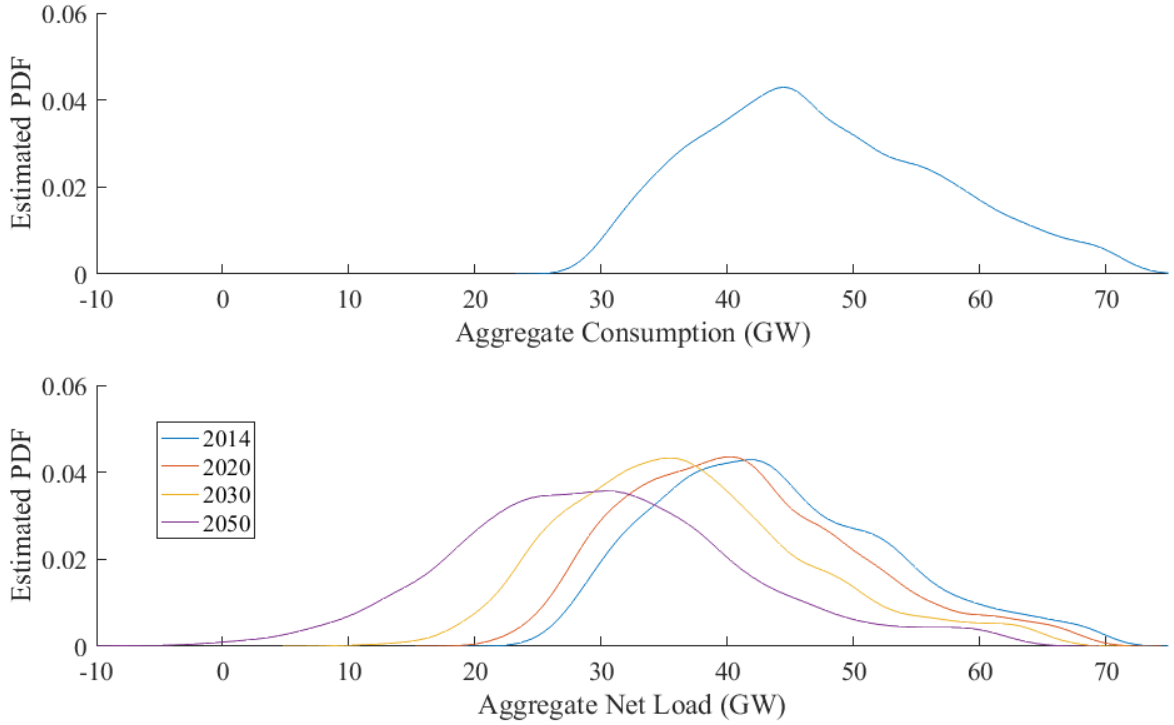

Fig. 13. Estimated PDFs of the hourly aggregate 2012 consumption, and of the net load in the different scenarios (using 2012 meteorological year for the VRE generation simulations).

TABLE VII. DESCRIPTIVE STATISTICS FOR THE AGGREGATE CONSUMPTION AND NET LOAD IN THE SCENARIOS

Scenario	Mean (GW)	STD (GW)	RSD	5th percentile (GW)	95th percentile (GW)
Only consumption	47.3	9.5	0.20	33.1	64.8
2014	43.8	9.4	0.22	30.2	61.9
2020	41.2	9.4	0.23	28.0	59.8
2030	36.9	9.9	0.27	23.0	56.2
2050	30.0	11.5	0.38	12.1	50.9

The first row describes the variability in the 2012 aggregate consumption (on average for the whole year on hourly resolution). The other rows describe the ramp rates in the aggregate net load in the different scenarios (using the 2012 meteorological year for the VRE generation simulations).

5.3. Ramp Rates of the Net Load

The estimated PDFs of the 1st differences of aggregate consumption (for 2012) and the net load are presented in Fig. 14, with descriptive statistics shown in Table VIII. The high positive ramp rates, around 4 GW, in the aggregate consumption relate to the working day morning up ramping (also visible in Fig. 12).

As can be seen in Fig. 14 and Table VIII, the major source of hourly changes in the aggregate net load in all scenarios is consumption. This is in line with the scatter plots shown in Fig. 8 and Fig. 12, with higher correlation of consecutive hours in the aggregate VRE generation than in the aggregate consumption. The VRE generation causes a significant increase in the hourly ramp rates only in the 2050 scenario.

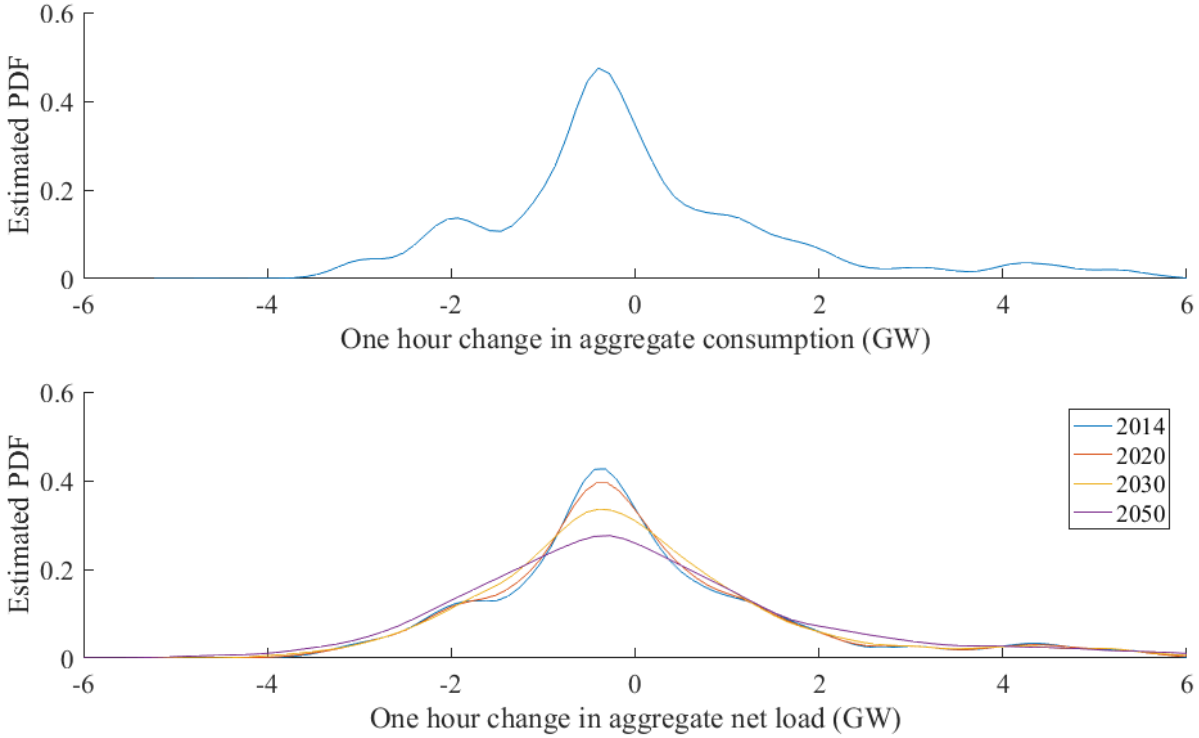

Fig. 14. The top subplot shows the estimated PDF of the 1st difference of the aggregate hourly consumption for 2012. The bottom subplot shows the estimated PDFs of the 1st differences of the aggregate net load (aggregate consumption subtracted by the aggregate VRE generation) in the different scenarios (using 2012 meteorological year for the VRE generation simulations).

TABLE VIII. DESCRIPTIVE STATISTICS FOR THE 1ST DIFFERENCE OF THE AGGREGATE CONSUMTION AND NET LOAD IN THE SCENARIOS

Scenario	STD (GW)	5th percentile (GW)	95th percentile (GW)
Only consumption	1.63	-2.28	3.62
2014	1.63	-2.29	3.62
2020	1.63	-2.29	3.57
2030	1.66	-2.34	3.58
2050	1.86	-2.62	3.75

The first row describes ramp rates in 2012 aggregate consumption (on average for the whole year on hourly resolution). The other rows describe ramp rates in the aggregate net load in the different scenarios (using the 2012 meteorological year for the VRE generation simulations).

6. FORECASTING ERRORS IN WIND GENERATION

This section presents the adjustment algorithm for combining meteorological wind generation forecasts and the predictive power of previous measured wind generation values. The algorithm is then applied to estimate 5 minute, 15 minute and one hour ahead forecasting uncertainties in the scenarios. All analyses are carried out using 5 minute resolution data.

6.1. Adjustment Algorithm for Wind Generation Forecasts

It is assumed in CorWind that the meteorological (MET) forecast is updated every 6 hours. Because of the high autocorrelation in wind generation, as seen in Fig. 7 and, for example, in [2], [3], the previous measured wind generation values can also be used in wind generation forecasts. The adjustment algorithm is used to combine the predictive power of the MET forecast and the previous measured wind generation values in an optimal way. The adjustment is done for each analysed area separately.

The adjusted wind generation forecast for time t for an area i is

$$\hat{p}_{i,t} = w_{\mathrm{AR};i,d}\hat{p}_{\mathrm{AR};i,t} + w_{\mathrm{MET};i,d}x_{i,t}, \tag{3}$$

where $\hat{p}_{\mathrm{AR};i,t}$ is the autoregressive (AR) forecast and $x_{i,t}$ is the MET forecast for t; the weights $w_{\mathrm{AR};i,t}$ and $w_{\mathrm{MET};i,t}$ depend on how far to the future the forecast is calculated (this is denoted by d).

The AR model parameters were estimated from the first two years of the simulated wind generation data for the different areas

using the 5 minute resolution data. The order for the AR models was selected as 4 for all areas (MA parts were not included, as the residuals of the AR(4) models did not show significant autocorrelation for any area). The MET forecasts are given by the CorWind model, as was explained in Section 2.2.

The weights $w_{\mathrm{AR};i,t}$ and $w_{\mathrm{MET};i,t}$ were estimated for different delays d by fitting a regression model

$$p_{i,t} = w_{\mathrm{AR};i,d}\hat{p}_{\mathrm{AR};i,t} + w_{\mathrm{MET};i,d}x_{i,t} + e_{i,t}, \tag{4}$$

where $p_{i,t}$ is the simulated wind generation for area i, the weights are the coefficients to be estimated, $\hat{p}_{\mathrm{AR};i,t}$ and $x_{i,t}$ are the explanatory variables ($\hat{p}_{\mathrm{AR};i,t}$ is calculated using the estimated AR model using d steps old data) and $e_{i,t}$ is the error term of the model. The model was estimated using OLS. The resulting estimated weights can be seen in Fig. 15.

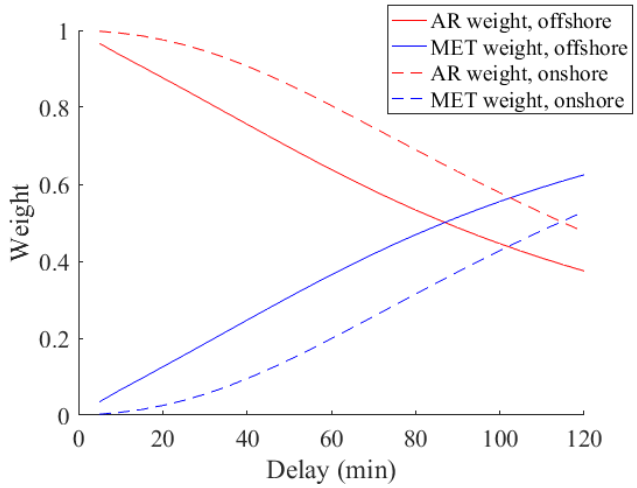

Fig. 15. The estimated weights for the AR and MET models in the adjustment algorithm for different delays. The presented values are the averages of the estimated weights for the individual areas (divided to onshore and offshore wind generation).

6.2. Differences between Onshore and Offshore Wind Generation

As seen in Fig. 15, for small delays the adjustment algorithms for both onshore and offshore wind generation rely heavily on the previous measured wind generation values. When the delay grows, the MET forecasts become more important, and for a 2 hours-ahead forecasting the adjustment algorithms for both types rely more on the MET forecasts. Overall, the adjustment algorithms for offshore wind generation rely more on the MET forecasts (another way to look at this is that, on average, the predictive power of the previous generation values is not as great with offshore wind generation, as it is with onshore wind generation). The differences between the variability of offshore and onshore wind generation are in line with previous studies, such as [11].

Examples of the resulting forecasts for an onshore and offshore location are shown in Fig. 16. The calm behaviour (i.e., very few or no sudden changes) of the simulated PIC wind generation allows the 5 and 15 minute ahead forecasts to be very accurate for the onshore locations. For the offshore location, the 5 and 15 minute ahead forecasts show more uncertainty. The same difference can be seen in Appendix C: the forecast error STDs are significantly lower for the onshore locations than for the offshore locations for 5 and 15 minute ahead forecasts. For hour ahead forecasts the differences are smaller; however, onshore locations still show lower forecast error STDs.

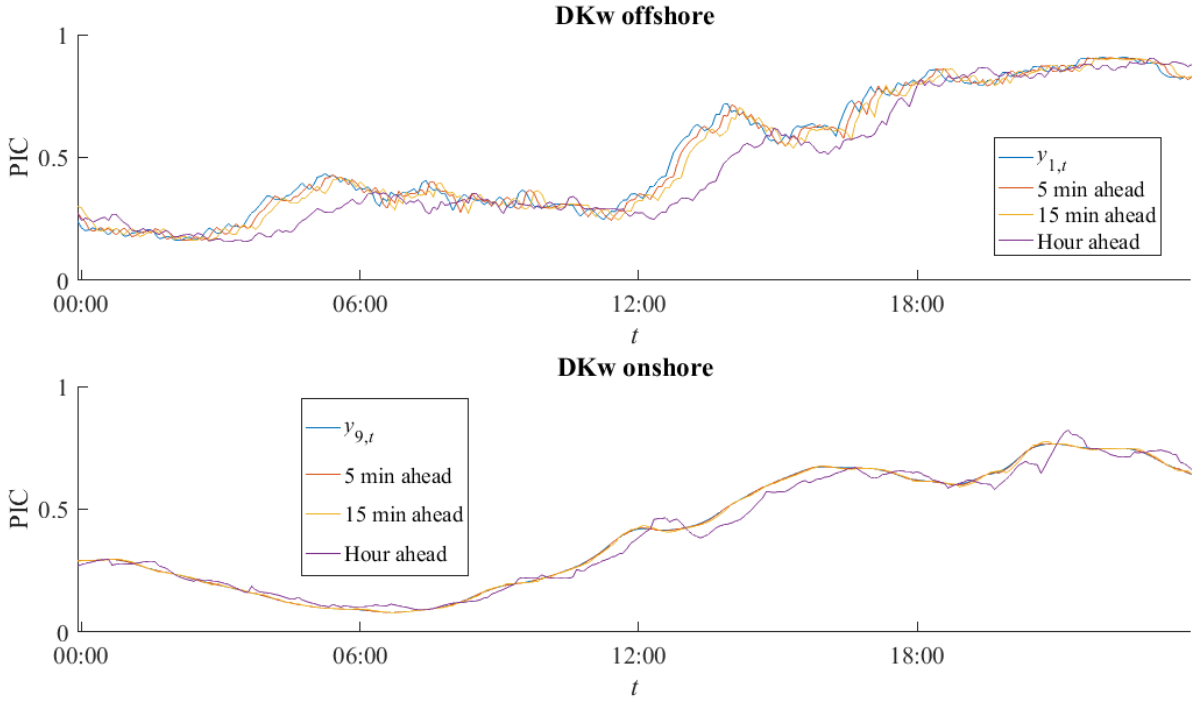

Fig. 16. Example time series of the simulated 5 minute resolution offshore and onshore wind generation with the 5 minute, 15 minute and one hour ahead simulated forecasts (using the estimated adjustment algorithm) for one day. An additional delay of 5 minutes was added for all cases to represent the delay in acquiring and analysing the data. The forecasts are continually updated.

6.3. Comparison to Persistence Forecasts

Table IX presents a comparison of the adjustment algorithms (each area has its own adjustment algorithm weights) to persistence forecasts (i.e., using the latest available value as a prediction to all future time steps). It can be seen that the adjustment algorithm provides significantly lower standard deviations of the forecast errors for all tested cases. Results for each individual area can be seen in Appendix C.

TABLE IX. STANDARD DEVIATIONS OF THE FORECAST ERRORS OF AGGREGATE WIND GENERATION IN 2014 USING TWO DIFFERENT FORECASTING METHODS

Method	5 min ahead	15 min ahead	Hour ahead
Persistence	0.0040	0.0075	0.0221
Adjustment	0.0021	0.0034	0.0116

The STD estimates are for PIC data, with 5 minute resolution. An additional delay of 5 minutes was added for all tested cases to represent delay in acquiring and analysing the data. Results for each individual area can be seen in Appendix C. An additional delay of 5 minutes was added for all tested cases to represent the delay in acquiring and analysing the data. The forecasts were continually updated.

6.4. Forecasting Uncertainties in the Scenarios

The STDs of the 5 minute, 15 minute and 1 hour ahead forecast errors of aggregate PIC wind generation are presented in Table X. It can be seen that the STDs of the 5 and 15 minute ahead forecasting errors increase slightly when going from 2014 to 2020, even though the geographical dispersion of the installed wind generation capacity increases; this is because of the higher share of offshore wind generation (see Section 6.2, and Table I). The STD of the hour ahead forecasting error decreases from 2014 to 2020 (thus, in hour ahead forecasting the increased geographical distribution seems to be more significant than the higher share of offshore wind generation).

Going from 2020 to 2050, the STDs of the 5 and 15 minute ahead PIC wind generation forecasting errors decrease, which is expected as the share of offshore wind generation decreases (Table I). The STD of the hour ahead forecasting errors decreases slightly when going from 2020 to 2030, and then increases slightly in 2050. It is difficult to pinpoint what causes these small changes, however the changes are similar as with the STD of the one-hour ramp rates shown in Table VI.

Table XI broadens the perspective from looking only at STDs to also looking at the tails of the forecasting error PDs (this is done only for 2014; however the same observations are true for the other scenarios as well). The relatively high kurtosis values imply that the forecasting error PDs are fat-tailed, i.e., the probabilities of very low or high forecast errors are higher than a normal distribution would predict. This means that while most of the time the adjustment algorithm can forecast wind generation well, there are some instances when the forecasts are significantly wrong. Examples on how the normal distribution would give

too low probabilities for the very low and high percentiles are given in Table XI. The kurtosis values for the forecast errors in the individual areas are even higher than for the aggregate wind generation.

TABLE X. STANDARD DEVIATIONS OF THE FORECAST ERRORS OF AGGREGATE WIND GENERATION IN THE SCENARIOS USING THE ADJUSTMENT ALGORITHM

Scenario	5 min ahead	15 min ahead	Hour ahead
2014	0.0021	0.0034	0.0116
2020	0.0023	0.0036	0.0100
2030	0.0015	0.0027	0.0092
2050	0.0012	0.0025	0.0104

The estimates STDs are for aggregate PIC data, with 5 minute resolution. An additional delay of 5 minutes was added for all tested cases to represent delay in acquiring and analysing the data. The forecasts were continually updated.

TABLE XI. DIFFERENT PERCENTILES OF THE FORECAST ERRORS OF AGGREGATE WIND GENERATION IN 2014 USING THE ADJUSTMENT ALGORITHM

Percentile	5 min ahead	15 min ahead	Hour ahead
5^{th}	-0.0034 (-0.0034)	-0.0057 (-0.0057)	-0.0191 (-0.0191)
95^{th}	0.0034 (0.0034)	0.0056 (0.0057)	0.0191 (0.0191)
0.1^{st}	-0.0079 (-0.0064)	-0.0131 (-0.0106)	-0.0443 (-0.0359)
99.9^{th}	0.0079 (0.0064)	0.0136 (0.0106)	0.0454 (0.0359)
Kurtosis	4.58	4.75	4.60

The estimates are for aggregate PIC data, with 5 minute resolution. The value in the brackets is the corresponding percentile of a normal distribution (fitted to the corresponding forecast errors). The last row shows the estimated kurtosis of the forecasts errors. The forecasts were continually updated.

7. ADDITIONAL NEEDS FOR FLEXIBILITY IN THE SCENARIOS

This section presents the needs for flexibility caused by the variability in VRE generation presented in Section 5, and by the uncertainty in wind generation forecasts presented in Section 6.

7.1. Hourly Variability in the Net Load

Section 5.2 described the expected variability in the aggregate net load in the different scenarios (using 2012 consumption). The STD of the aggregate net load is not changing much until 2050, when there is a modest increase. However, the mean of net load decreases. Thus, there will be less energy to be generated by the other generation types, such as hydro power, while the need for flexibility increases (i.e., the RSD of the net load will increase significantly). In addition to the other generation types, flexibility can also be acquired from the demand side, by transferring the generated power to neighbouring countries or by storing energy (Section 7.4 describes how the presented results will be used further in the Flex4RES project to compare these options).

In addition to its STD, the shape of the net load PD in Fig. 13 requires attention when considering the need for flexibility. The probability of reaching a very high net load decreases (because there is usually some VRE generation available during the highest consumption hours); however, there is always some probability that VRE generation is zero, and thus the net load can reach very high values (i.e., the highest possible net load is determined by peak consumption). This can lead to a situation where, for some operators, there is little incentive to hold enough other generation capacity to meet the very rare peak net load.

7.2. Hourly Ramp Rates of the Net Load

As was shown in Section 5.3, the hourly ramp rates of the aggregate net load are caused mainly by consumption. Thus, when looking on average at all the hours of the year, the increasing share of VRE generation is not likely to increase the hourly ramp rates significantly (although some increase is expected in the 2050 scenario). However, the hourly changes in consumption are usually known well in advance (such as the ramping up in working day mornings). For wind generation, however, the hourly changes can happen at any hour of the day. For solar generation, the changes in generation during the day are more predictable; however, as the installed solar generation capacity is very low in the scenarios (Table I), the aggregate VRE generation follows mostly the behaviour of wind generation. This has a possible effect on the flexibility needs: even though on average the amount of required flexibility for one-hour changes in not significantly increased, the time when the flexibility is needed is more uncertain.

7.3. Uncertainty in Wind Generation Forecasts

Looking at Table X, the STDs of the short term (5 or 15 minutes ahead) forecasting errors are expected to be less than 0.4% of the installed wind generation capacity for all scenarios. For hour ahead forecasting (which on 5 minute resolution means

forecasting the 5 minute average wind generation after one hour), the expected STDs of the forecast errors are around 1% of the installed wind generation capacity for all scenarios.

The relatively high kurtoses of the forecasting error PDs (Table XI) have to be emphasized: the risk of experiencing a much greater forecasting error (an "outlier") is higher than what one would expect assuming normality. These events are often related to storms; this is discussed more in Section 8.3. Also, when considering 5 minute data, the 0.1st or 99.9th percentiles, which may sound "unlikely", depict events that are actually not that rare. During one (non-leap) year, there are 8760×12 time steps on 5 minute resolution. Out of these, around 100 time steps belong to the 0.1st percentile (and similarly to the 99.9th percentile). The hour ahead forecasting error is thus expected to be greater than 4% of the aggregate installed wind generation capacity many times during a year (see Table XI).

To understand the effects of the above mentioned expected uncertainties in wind generation forecasting on the required power system reserves, they have to be compared to the current and planned reserves. Due to time limitations, this is left for future work; this is discussed more in Section 8.7. Also, the forecasting error modelling should be expanded to consider solar generation; this is discussed in Section 8.4.

7.4. Using the Presented Time Series and Results in Further Studies

There are many ways of providing the additional flexibility required by the increasing share of VRE generation, e.g., flexibility from other generation types (such as hydro power), demand-side response, and transmission of power to or from surrounding countries. However, this report does not judge which of the different sources of flexibility are the most suitable; the other parts of the Flex4RES project aim to do this. The hourly solar and wind generation time series, and the forecasting error time series, are available for all the partners in the project to help to achieve this goal.

The following section presents the planned additions to the presented VRE simulation methodology to provide simulated time series that even more accurately describe the variability of the studied VRE generation and its uncertainties. These additions are planned to be carried out during the Flex4RES, and the time series acquired using the updated methodology are available to all partners of the project.

8. Discussion and Future Work

This section provides further discussions on some of the important aspects of the presented methodology, explains the planned updates to the presented VRE simulation methodology and discusses the future work.

8.1. Changing the Geographical Distributions of Installed VRE Generation within the Analysed Areas

As the installed VRE generation increases in an area, the relative geographical distribution will change, at least somewhat. If the new generation is installed to locations within the area with no or very little current installed capacity, the area's STD (as shown in Appendix A for the current installation) should decrease. However, if the new generation is installed, for example, as a very large unit in a single location within the area, the STD of the area's VRE generation may increase.

Analysing the changes in the geographical distribution of the installed VRE generation within the analysed areas is one of the most important updates to the presented methodology. It will be carried out by using the most recent information on the planned installations from different sources. All planned VRE generation installations with known geographical locations will be put in a database, and this information will be used to provide the geographical distribution of the installed VRE generation for each scenario (offshore wind generation shall be analysed even on the level of individual wind farms).

8.2. Changing Wind Generation Power Curves in the Future Scenarios

For example in [12], it is mentioned that the power curves can be more efficient for future installed wind generation (especially for low-wind onshore sites). This would mean getting more power with the same wind speed, and would increase the capacity factor of the wind generation. As described in Section 2.2, the presented methodology allows different power curves to be set for different locations. Thus, the effects of the changes in power curves can be modelled with the methodology; however, it requires the modelling of the expected change in the curves.

8.3. Assessment of the Adjustment Algorithm with Measured Wind Generation Data

All the presented results will be compared to measured data (for the 2014 scenario). Especially important is to test the adjustment algorithm, as it is a new addition to the CorWind program. Its behaviour should be inspected especially in storm cases, i.e., in cases when there is a significant risk that most of the wind farms in a given area experience so high wind speeds that they will be shut down. In such cases the previous measured wind generation values may not be reliable in forecasting the future wind generation values.

8.4. Solar Generation Forecasting Error Modelling

The forecast error modelling will be extended from wind generation to also cover solar generation. As was explained in Section 3.3, part of the variability in solar generation is caused by deterministic factors, which means that a significant part of the variability in solar generation should be highly predictable. The two parts of wind generation forecasting were presented in 6.1:

the MET and the AR forecast. The AR model estimation should be possible also for solar generation, following, for example, the approach presented in [4] for modelling irradiance data. The plan is also to get data about the MET forecast uncertainties for solar power.

8.5. Solar Irradiance to Power Modelling

The solar generation simulation framework shown in Fig. 3 allows for a very accurate irradiation to power modelling. Theoretically, different tilt angles (or sun tacking systems) can be specified for individual locations. However, in reality measured data is usually available only on aggregated levels with different panel set ups in the mix. Thus, in future work the aim is to generate simple but representative irradiance to power models for such large aggregate areas. However, these models could still be extended to include, for example, ambient temperature and wind speed data.

8.6. Using More Consumption and Meteorological Data

The results presented in Section 4 are based on five meteorological years (from 2011 to 2015). To provide more accurate estimates, more simulation years will be considered when carrying out the simulations with the updated methodology in the future. However, the greatest uncertainties are in the results presented in Section 5, as the estimates relating to the aggregate net load are based only one single year's consumption data. One year of consumption data is clearly not enough for estimating the very lowest and highest percentiles of the net load, i.e., for estimating the probabilities of having simultaneously very high consumption and low VRE generation, or vice versa (for this reason, only 5th and 95th percentiles are presented in Tables VII and VIII).

The challenges of estimating the very lowest and highest percentiles of the net load can be seen in Fig. 17. The highest consumption occurs on very specific hours of the year (in the Nordic and Baltic countries usually during the coldest days). To estimate, for example, the risk of simultaneously having high consumption and low VRE generation, a lot of data is needed [10]. If consumption data is not available from many years, an alternative is to estimate stochastic models for consumption in the different analysed countries and use these models to generate simulated consumption time series (as was done, for example, in [10]). However, consumption modelling is outside of the scope of this paper, so it is not considered further.

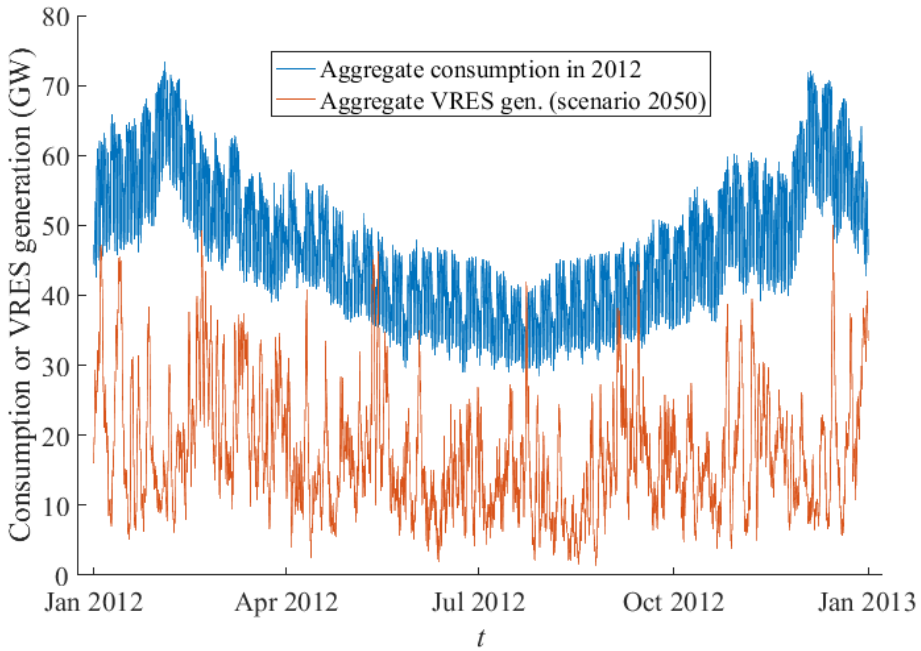

Fig. 17. Aggregate hourly consumption time series of 2012 and aggregate hourly VRE generation for the 2050 scenario (using the 2012 meteorological year).

8.7. Comparing the Uncertainties in VRE Generation Forecasts to the Available Power System Reserves

To understand the expected effects of the uncertainties in wind generation forecasts to power system reserves (10 minute reserves, emergency reserves, etc.), the results presented in this paper have to be compared to the existing and planned reserves. To understand the order of magnitude of the challenge, the uncertainties should also be compared to other sources of reserve needs (for example, to the size of the largest generation unit in the power system). However, due to time limitations, these comparisons are left for future work.

8.8. Modelling Less Aggregated Areas

The results in this paper are presented for the aggregated VRE generation and consumption of all the areas included in the

analyses. This corresponds to the case when there are no bottle necks in the power system, and all VRE generation can be transferred to where there is consumption. However, the presented methodology can also be used to model smaller geographical areas by aggregating less (for example, only one country).

8.9. Modelling More Countries

This paper has focused on Nordic and Baltic countries, as they are focus of the Flex4RES project. However, the presented methodology can be used to simulated VRE generation also in other countries (as long as data is available). The VRE generation of the relevant surrounding countries will also be simulated to be used in the Flex4RES project.

8.10. Assessing the Analysed Scenarios

The scenarios (i.e., the installed capacities on the different VRE generation types in the different areas) analysed in this paper are the baseline scenarios from [1]. In some aspects, these scenarios differ significantly from the European Wind Energy Association's (EWEA) latest scenarios [13]. It is advised that in the future work the scenarios are compared and assessed against the newest EWEA scenarios (and other sources, especially considering the installed solar generation).

9. Conclusion

This paper has presented estimates of the variability in wind and solar generation in the 2020, 2030 and 2050 (and 2014) scenarios specified in [1]. Considering the needs for flexibility, the findings can be summarized as follows. Compared to the hourly ramp rates in consumption, the increasing VRE generation does not significantly increase the hourly ramp rates in the aggregate net load in any scenario. There is some increase in the 2050 scenario; however, it is still relatively modest (the aggregate net load ramp rate STD in 2050 is expected to be 14% higher than in 2014).

The STD of the aggregate hourly net load increases slightly in 2030, and notably in 2050 (it is estimated to be 22% higher in 2050 than in 2014). At the same time, the mean of net load decreases. Thus, there will be less energy to be generated by the other generation types, such as hydro power, while the need for flexibility increases (i.e., the RSD of the net load will increase significantly). Alternatively, the variability in the net load can be managed by demand-side response, transmission of power to or from surrounding countries or by storing energy.

With more VRE generation installed, the probability of very high net load decreases (as some VRE generation is usually available during peak consumption). However, there is always some probability that the aggregate VRE generation is zero, and thus the highest possible net load is determined by peak consumption. This may raise questions considering the incentives to hold enough other generation capacity to meet the rare peak net load. The presented methodology can be used to estimate the probability of reaching a very high aggregate net load; however, such analysis needs more data.

It was shown that the relative forecasting errors are generally lower for onshore than for offshore wind generation. Using 5 minute resolution, the STDs of the short term (5 or 15 minute ahead) forecasting errors are less than 0.4% of the installed aggregate wind generation capacity, and the STDs of the hour ahead forecasting errors around 1% of the installed aggregate wind generation capacity for all scenarios. The forecasting error PDs are fat-tailed, which means that the risk of experiencing a large forecasting error (an "outlier") is higher than what one would expect assuming normality. The modelling of solar forecasting errors, and the comparison of the forecasting uncertainties to the available and planned power system reserves are left for future work.

In addition to the estimated needs for flexibility in the analysed scenarios, it was shown that the geographical distribution of installed VRE generation has a significant effect on the PD of the aggregate VRE generation. In the analysed scenarios, the geographical dispersion increases significantly when going from 2014 to 2020, which decreases the relative variability. When going from 2020 to 2030 and to 2050, the overall geographical distribution does not change significantly, which leads to similar relative variabilities in the 2020, 2030 and 2050 scenarios.

It was shown that the correlation between solar and wind generation is generally slightly negative, which might reduce the variability of the aggregate VRE generation compared to only having wind generation in the VRE generation mix (however, the installed solar generation capacities are very low in the analysed scenarios). It is important to note that while the described dependency structure applies on average throughout the year, during a storm the situation can be the opposite: wind generation may need to be shut down because of too high wind speeds and solar generation may be zero because of the storm clouds (i.e., positive correlation). As was mentioned before, there is always some probability of the aggregate VRE generation being zero.

Acknowledgment

The research was funded by the Flex4RES - Flexible Nordic Energy Systems project. The authors would also like to thank Thure Traber from DTU Department of Management Engineering for providing the area-wise installed VRE capacities used in [1] and for compiling the hourly consumption data set for 2012 from ENTSO-E [9].

REFERENCES

[1] Nordic Energy Technology Perspectives 2016: http://www.nordicenergy.org/project/nordic-energy-technology-perspectives/ (accessed on September 28th, 2016).

[2] M. Koivisto, J. Ekström, J. Seppänen, I. Mellin, J. Millar, L. Haarla, "A Statistical Model for Comparing Future Wind Power Scenarios with Varying Geographical Distribution of Installed Generation Capacity", *Wind Energy*, vol. 19, no. 4, April 2016 (http://dx.doi.org/10.1002/we.1858).

[3] J. Ekström, M. Koivisto, I. Mellin, J. Millar, E. Saarijärvi, L. Haarla, "Assessment of Large Scale Wind Power Generation with New Generation Locations without Measurement Data", *Renewable Energy*, vol. 83, pp. 362-374, November 2015 (http://dx.doi.org/10.1016/j.renene.2015.04.050).

[4] J. Ekström, M. Koivisto, J. Millar, I. Mellin, and M. Lehtonen, "A statistical approach for hourly photovoltaic power generation modeling with generation locations without measured data," *Solar Energy*, vol. 132, pp. 173 – 187, 2016 (http://dx.doi.org/10.1016/j.solener.2016.02.055).

[5] M. Marinelli, P. Maule, A. N. Hahmann, O. Gehrke, P. B. Nørgård, and N. A. Cutululis, "Wind and photovoltaic large-scale regional models for hourly production evaluation", *IEEE Transactions on Sustainable Energy*, vol. 6, no. 3, pp. 916–923, July 2015 (http://dx.doi.org/10.1109/TSTE.2014.2347591).

[6] ENTSO-E Policy Brief February 2015: https://www.entsoe.eu/Documents/Publications/Position%20papers%20and%20reports/150210_ENTSO-E_Policy_paper_Energy_mix.pdf (accessed September 28th, 2016).

[7] Nord Pool bidding areas: http://www.nordpoolspot.com/How-does-it-work/Bidding-areas/ (accessed September 28th, 2016).

[8] X. Larsén, S. Ott, J. Badger, A. Hahmann, and J. Mann, "Recipes for Correcting the Impact of Effective Mesoscale Resolution on the Estimation of Extreme Winds," *American Meteorology Society*, vol. 51, p. 521–533, 2012.

[9] ENTSO-E hourly consumption data for 2012; available through: https://www.entsoe.eu/data/data-portal/consumption/Pages/default.aspx

[10] M. Koivisto, M. Degefa, M. Ali, J. Ekström, J. Millar, M. Lehtonen, "Statistical Modeling of Aggregated Electricity Consumption and Distributed Wind Generation in Distribution Systems Using AMR Data", *Electric Power Systems Research*, vol. 129, pp. 217–226, December 2015 (http://dx.doi.org/10.1016/j.epsr.2015.08.008).

[11] P. Sørensen, N. Cutululis, A. Vigueras-Rodriguez, L. Jensen, J. Hjerrild, M. Donovan and H. Madsen, "Power Fluctuations from Large Wind Farms," *IEEE Transactions on Power Systems*, 2007.

[12] EurObserv'ER Wind energy barometer 2016: http://www.eurobserv-er.org/wind-energy-barometer-2016/ (accessed September 28th, 2016).

[13] European Wind Energy Association's Wind energy scenarios for 2030: http://www.ewea.org/fileadmin/files/library/publications/reports/EWEA-Wind-energy-scenarios-2030.pdf (accessed September 30th, 2016).

APPENDIX A: INSTALLED WIND AND SOLAR GENERATION CAPACITIES IN THE DIFFERENT SCENARIOS

	Offshore wind								Onshore wind																Solar														
Scenario	**DKw**	**DKe**	**SE**	**FI**	**EE**	**LV**	**LT**	**NO**	**DKw**	**DKe**	**SE1**	**SE2**	**SE3**	**SE4**	**FIs**	**FIn**	**EE**	**LV**	**LT**	**NO1**	**NO2**	**NO3**	**NO4**	**NO5**	**DKw**	**DKe**	**SE1**	**SE2**	**SE3**	**SE4**	**FIs**	**FIn**	**EE**	**LV**	**LT**	**NO1**	**NO2**	**NO3**	**NO4**	**NO5**
2014	843	373	210	33	0	0	0	0	2946	583	387	1047	1620	1206	277	138	313	58	350	0	171	330	229	126	417	179	0	0	0	43	0	0	0	0	8	0	0	0	0	0
2020	1443	573	215	900	250	180	0	0	3345	724	387	1997	1620	1206	1067	533	400	570	500	124	171	330	2784	126	624	268	0	0	0	79	10	0	0	2	10	0	0	0	0	0
2030	1443	573	215	1206	250	180	0	0	4219	990	424	5488	4396	1206	1067	533	635	2979	1677	124	1410	330	5033	126	624	268	0	0	0	79	40	0	0	2	750	0	0	0	0	0
2050	1443	573	215	1206	250	180	0	0	6480	1520	5488	5488	10975	1206	1067	533	400	2409	7046	124	1410	5033	5033	126	624	268	0	0	0	79	40	0	0	2	740	0	0	0	0	0

The installed capacities in the scenarios are taken from the data used in [1] as the baseline scenarios. For onshore wind and solar Finland was divided into two areas (north and south), where the shares of the country-wise installed capacities are: onshore wind 1/3 to north and 2/3 to south; all solar to south.

Appendix B: PIC Generation Means, Standard Deviations and Correlations for the Simulated Hourly VRE Generation Data

		Offshore wind								Onshore wind																Solar															
	Area	DKw	DKe	SE	FI	EE	LV	LT	NO	DKw	DKe	SE1	SE2	SE3	SE4	FIs	FIn	EE	LV	LT	NO3	NO4	NO1	NO2	NO5	DKw	DKe	SE1	SE2	SE3	SE4	FIs	FIn	EE	LV	LT	NO3	NO4	NO1	NO2	NO5
	Mean	0.46	0.47	0.34	0.33	0.31	0.31	0.40	0.36	0.32	0.32	0.31	0.31	0.29	0.27	0.25	0.25	0.26	0.27	0.26	0.34	0.31	0.33	0.27	0.28	0.11	0.11	0.10	0.10	0.11	0.11	0.09	0.09	0.12	0.12	0.12	0.09	0.09	0.10	0.10	0.10
	STD	0.32	0.32	0.23	0.27	0.29	0.31	0.35	0.25	0.28	0.28	0.27	0.24	0.23	0.25	0.23	0.25	0.25	0.27	0.25	0.29	0.23	0.25	0.29	0.32	0.18	0.17	0.16	0.16	0.16	0.16	0.14	0.14	0.19	0.18	0.18	0.15	0.14	0.16	0.16	0.15
	RSD	0.69	0.68	0.68	0.83	0.94	1.01	0.86	0.69	0.88	0.88	0.87	0.79	0.80	0.92	0.92	0.98	0.94	0.98	0.98	0.85	0.74	0.75	1.06	1.15	1.55	1.53	1.65	1.60	1.56	1.55	1.62	1.64	1.56	1.53	1.54	1.61	1.63	1.59	1.60	1.58
	STD of diff	0.06	0.07	0.05	0.06	0.07	0.11	0.13	0.06	0.05	0.06	0.07	0.04	0.03	0.04	0.04	0.04	0.04	0.06	0.06	0.06	0.03	0.04	0.06	0.11	0.05	0.05	0.04	0.05	0.05	0.05	0.04	0.04	0.05	0.05	0.06	0.04	0.04	0.05	0.05	0.04

		Offshore wind								Onshore wind																Solar															
	Area	DKw	DKe	SE	FI	EE	LV	LT	NO	DKw	DKe	SE1	SE2	SE3	SE4	FIs	FIn	EE	LV	LT	NO3	NO4	NO1	NO2	NO5	DKw	DKe	SE1	SE2	SE3	SE4	FIs	FIn	EE	LV	LT	NO3	NO4	NO1	NO2	NO5
Offshore wind	DKw		0.73	0.65	0.15	0.23	0.29	0.29	0.45	0.84	0.72	0.04	0.15	0.45	0.60	0.22	0.11	0.21	0.29	0.29	0.18	0.22	0.36	0.58	0.38	-0.13	-0.11	-0.13	-0.13	-0.13	-0.12	-0.12	-0.13	-0.12	-0.11	-0.10	-0.13	-0.12	-0.14	-0.16	-0.14
	Dke			0.81	0.13	0.25	0.35	0.37	0.30	0.76	0.88	0.04	0.13	0.47	0.76	0.20	0.09	0.23	0.35	0.38	0.13	0.18	0.30	0.44	0.22	-0.12	-0.11	-0.11	-0.11	-0.12	-0.12	-0.11	-0.11	-0.10	-0.09	-0.09	-0.10	-0.09	-0.11	-0.11	-0.11
	SE				0.43	0.44	0.49	0.46	0.41	0.72	0.79	0.22	0.42	0.73	0.84	0.46	0.37	0.40	0.50	0.47	0.28	0.32	0.49	0.42	0.28	-0.15	-0.14	-0.16	-0.16	-0.16	-0.15	-0.17	-0.17	-0.14	-0.13	-0.14	-0.16	-0.15	-0.16	-0.15	-0.16
	FI					0.45	0.31	0.24	0.30	0.15	0.13	0.52	0.61	0.44	0.17	0.73	0.91	0.47	0.31	0.20	0.37	0.42	0.37	0.07	0.18	-0.10	-0.10	-0.16	-0.14	-0.11	-0.11	-0.14	-0.16	-0.12	-0.11	-0.10	-0.15	-0.17	-0.11	-0.10	-0.12
	EE						0.69	0.56	0.26	0.26	0.26	0.17	0.38	0.60	0.35	0.68	0.33	0.85	0.74	0.55	0.28	0.19	0.36	0.12	0.14	-0.09	-0.09	-0.13	-0.13	-0.11	-0.11	-0.15	-0.15	-0.13	-0.12	-0.11	-0.14	-0.14	-0.10	-0.08	-0.11
	LV							0.75	0.24	0.33	0.36	0.10	0.27	0.55	0.46	0.46	0.23	0.62	0.89	0.74	0.23	0.15	0.30	0.16	0.13	-0.05	-0.05	-0.09	-0.09	-0.08	-0.07	-0.10	-0.09	-0.09	-0.08	-0.07	-0.09	-0.08	-0.05	-0.05	-0.07
	LT								0.21	0.31	0.35	0.08	0.23	0.47	0.44	0.35	0.18	0.49	0.76	0.83	0.19	0.14	0.27	0.16	0.10	-0.11	-0.12	-0.14	-0.14	-0.14	-0.13	-0.16	-0.15	-0.15	-0.14	-0.14	-0.15	-0.14	-0.11	-0.09	-0.12
	NO									0.43	0.32	0.19	0.32	0.44	0.33	0.30	0.26	0.25	0.25	0.20	0.73	0.55	0.59	0.60	0.65	-0.15	-0.14	-0.21	-0.20	-0.17	-0.15	-0.19	-0.21	-0.16	-0.15	-0.15	-0.21	-0.22	-0.19	-0.20	-0.22
Onshore wind	DKw										0.84	0.03	0.17	0.52	0.73	0.24	0.12	0.24	0.35	0.34	0.18	0.20	0.38	0.63	0.38	-0.05	-0.04	-0.06	-0.06	-0.06	-0.05	-0.08	-0.08	-0.05	-0.04	-0.06	-0.07	-0.04	-0.07	-0.05	-0.06
	DKe											0.04	0.15	0.50	0.81	0.21	0.10	0.25	0.38	0.40	0.13	0.17	0.31	0.48	0.25	-0.05	-0.05	-0.05	-0.06	-0.05	-0.06	-0.07	-0.07	-0.04	-0.04	-0.05	-0.05	-0.03	-0.05	-0.04	-0.04
	SE1												0.53	0.19	0.05	0.30	0.57	0.19	0.12	0.08	0.27	0.46	0.26	0.02	0.08	-0.11	-0.11	-0.17	-0.14	-0.12	-0.11	-0.14	-0.16	-0.12	-0.12	-0.12	-0.15	-0.20	-0.11	-0.10	-0.12
	SE2													0.52	0.20	0.58	0.55	0.39	0.30	0.22	0.44	0.37	0.59	0.06	0.14	-0.07	-0.07	-0.13	-0.12	-0.09	-0.07	-0.13	-0.15	-0.10	-0.09	-0.11	-0.15	-0.16	-0.09	-0.07	-0.10
	SE3														0.65	0.57	0.33	0.53	0.60	0.49	0.42	0.30	0.64	0.31	0.28	-0.14	-0.13	-0.17	-0.18	-0.16	-0.15	-0.20	-0.20	-0.16	-0.15	-0.16	-0.20	-0.17	-0.16	-0.14	-0.17
	SE4															0.27	0.13	0.31	0.50	0.51	0.17	0.19	0.35	0.46	0.22	-0.07	-0.07	-0.08	-0.08	-0.08	-0.07	-0.09	-0.09	-0.06	-0.06	-0.07	-0.08	-0.06	-0.07	-0.05	-0.07
	FIs																0.59	0.74	0.49	0.34	0.34	0.29	0.39	0.13	0.18	-0.06	-0.06	-0.11	-0.10	-0.08	-0.07	-0.12	-0.12	-0.09	-0.07	-0.07	-0.12	-0.12	-0.08	-0.06	-0.09
	FIn																	0.38	0.23	0.15	0.32	0.42	0.30	0.06	0.16	-0.08	-0.08	-0.13	-0.11	-0.09	-0.08	-0.12	-0.14	-0.09	-0.08	-0.08	-0.11	-0.15	-0.08	-0.07	-0.09
	EE																		0.68	0.52	0.28	0.19	0.33	0.13	0.13	-0.11	-0.11	-0.15	-0.14	-0.13	-0.12	-0.17	-0.17	-0.15	-0.13	-0.13	-0.16	-0.16	-0.11	-0.10	-0.13
	LV																			0.83	0.24	0.16	0.33	0.20	0.14	-0.05	-0.05	-0.09	-0.08	-0.07	-0.07	-0.11	-0.11	-0.09	-0.08	-0.08	-0.10	-0.09	-0.05	-0.04	-0.07
	LT																				0.17	0.13	0.26	0.21	0.11	-0.10	-0.11	-0.13	-0.13	-0.12	-0.12	-0.15	-0.14	-0.14	-0.13	-0.14	-0.14	-0.12	-0.10	-0.08	-0.11
	NO3																					0.53	0.59	0.15	0.31	-0.12	-0.12	-0.19	-0.18	-0.14	-0.13	-0.17	-0.19	-0.15	-0.14	-0.13	-0.21	-0.22	-0.14	-0.13	-0.18
	NO4																						0.39	0.24	0.32	-0.19	-0.19	-0.26	-0.24	-0.21	-0.20	-0.21	-0.24	-0.20	-0.19	-0.18	-0.23	-0.28	-0.21	-0.20	-0.22
	NO1																							0.29	0.41	-0.14	-0.13	-0.19	-0.19	-0.16	-0.14	-0.19	-0.20	-0.17	-0.16	-0.16	-0.24	-0.20	-0.18	-0.17	-0.21
	NO2																								0.54	-0.09	-0.08	-0.11	-0.10	-0.09	-0.08	-0.10	-0.11	-0.08	-0.07	-0.07	-0.09	-0.10	-0.12	-0.13	-0.12
	NO5																									-0.07	-0.06	-0.11	-0.10	-0.08	-0.06	-0.09	-0.11	-0.07	-0.06	-0.07	-0.10	-0.10	-0.12	-0.12	-0.12
Solar	DKw																										0.97	0.88	0.91	0.95	0.95	0.86	0.85	0.91	0.92	0.88	0.88	0.87	0.93	0.89	0.88
	DKe																											0.88	0.91	0.95	0.97	0.86	0.85	0.91	0.92	0.88	0.88	0.87	0.91	0.87	0.87
	SE1																												0.95	0.91	0.89	0.89	0.92	0.91	0.90	0.86	0.91	0.95	0.89	0.84	0.87
	SE2																													0.95	0.92	0.90	0.90	0.92	0.93	0.88	0.94	0.93	0.93	0.86	0.89
	SE3																														0.97	0.89	0.88	0.93	0.94	0.90	0.91	0.89	0.96	0.89	0.89
	SE4																															0.87	0.86	0.92	0.93	0.89	0.89	0.88	0.92	0.87	0.87
	FIs																																0.96	0.91	0.90	0.93	0.88	0.88	0.86	0.74	0.76
	FIn																																	0.89	0.88	0.91	0.88	0.91	0.85	0.74	0.77
	EE																																		0.98	0.91	0.90	0.90	0.89	0.84	0.86
	LV																																			0.94	0.91	0.90	0.90	0.85	0.87
	LT																																				0.87	0.86	0.86	0.75	0.77
	NO3																																					0.92	0.91	0.83	0.90
	NO4																																						0.86	0.82	0.85
	NO1																																							0.90	0.91
	NO2																																								0.95
	NO5																																								

The presented values are calculated using all the five years of simulated hourly VRE generation data.

APPENDIX C: PIC FORECAST ERROR STANDARD DEVIATIONS AND CORRELATIONS FOR THE SIMULATED 5 MINUTE RESOLUTION 2014 WIND GENERATION DATA

		Offshore wind								Onshore wind															
Delay	**Area**	**DKw**	**DKe**	**SE**	**FI**	**EE**	**LV**	**LT**	**NO**	**DKw**	**DKe**	**SE1**	**SE2**	**SE3**	**SE4**	**FIs**	**FIn**	**EE**	**LV**	**LT**	**NO3**	**NO4**	**NO1**	**NO2**	**NO5**
5 min	**Persistence**	0.023	0.022	0.023	0.025	0.026	0.048	0.063	0.026	0.009	0.011	0.014	0.007	0.005	0.008	0.007	0.008	0.007	0.011	0.012	0.011	0.005	0.007	0.013	0.039
ahead	**Adjustment**	0.022	0.021	0.023	0.024	0.025	0.047	0.061	0.026	0.002	0.003	0.005	0.001	0.001	0.002	0.001	0.002	0.002	0.003	0.003	0.003	0.002	0.001	0.004	0.037
15 min	**Persistence**	0.034	0.034	0.033	0.035	0.039	0.068	0.087	0.037	0.017	0.022	0.027	0.013	0.011	0.016	0.013	0.016	0.015	0.022	0.023	0.022	0.010	0.014	0.026	0.061
ahead	**Adjustment**	0.032	0.032	0.032	0.034	0.037	0.066	0.083	0.035	0.005	0.008	0.012	0.003	0.003	0.004	0.004	0.005	0.004	0.010	0.009	0.009	0.004	0.004	0.012	0.057
Hour	**Persistence**	0.072	0.072	0.058	0.067	0.081	0.120	0.146	0.066	0.052	0.062	0.075	0.041	0.033	0.047	0.040	0.048	0.045	0.063	0.063	0.063	0.030	0.042	0.072	0.122
ahead	**Adjustment**	0.062	0.061	0.050	0.057	0.070	0.106	0.125	0.056	0.028	0.041	0.050	0.018	0.013	0.025	0.019	0.026	0.023	0.043	0.043	0.038	0.015	0.020	0.050	0.100

		Offshore wind								Onshore wind															
	Area	**DKw**	**DKe**	**SE**	**FI**	**EE**	**LV**	**LT**	**NO**	**DKw**	**DKe**	**SE1**	**SE2**	**SE3**	**SE4**	**FIs**	**FIn**	**EE**	**LV**	**LT**	**NO3**	**NO4**	**NO1**	**NO2**	**NO5**
Offshore wind	**DKw**		0.08	0.04	0.02	0.00	-0.01	-0.01	0.01	0.11	0.05	-0.01	0.00	0.00	0.00	0.00	-0.01	0.00	-0.01	-0.01	-0.01	0.00	0.01	0.03	0.00
	DKe			0.18	0.04	0.02	0.00	0.01	-0.02	0.02	0.22	0.01	0.01	0.01	0.07	0.02	0.03	0.02	0.02	0.03	-0.03	0.00	0.03	0.01	-0.01
	SE				0.04	0.02	-0.01	0.00	0.00	0.04	0.07	0.00	0.03	0.04	0.12	0.04	0.04	0.03	-0.01	0.00	0.00	0.01	0.01	0.02	0.00
	FI					-0.01	0.00	0.02	0.01	0.00	0.01	0.03	0.02	0.01	0.01	0.09	0.39	0.03	-0.01	0.02	-0.01	-0.01	0.01	0.01	0.01
	EE						0.06	0.03	-0.02	0.00	0.00	-0.01	-0.01	0.01	-0.01	0.01	-0.01	0.12	0.04	0.02	0.01	-0.01	0.03	-0.01	0.01
	LV							0.11	-0.03	0.01	0.00	-0.02	0.00	-0.01	0.00	0.01	0.00	0.03	0.28	0.09	0.00	0.00	0.01	0.00	0.01
	LT								0.00	0.01	-0.01	0.00	-0.02	0.00	0.02	0.02	0.01	0.00	0.07	0.18	-0.01	0.00	0.01	-0.01	0.02
	NO									0.03	-0.02	0.01	0.00	0.00	0.00	0.01	-0.02	0.01	-0.02	-0.02	0.08	-0.01	-0.03	0.19	0.08
Onshore wind	**DKw**										0.06	0.00	0.03	0.03	0.02	0.03	0.00	0.02	0.04	0.01	-0.02	-0.01	0.03	0.05	0.02
	DKe											0.03	0.00	0.04	0.06	0.01	-0.01	0.01	0.01	0.03	0.00	0.02	0.01	0.01	0.01
	SE1												0.02	0.01	-0.02	0.01	0.04	0.02	-0.01	0.01	0.01	0.02	0.03	-0.01	-0.01
	SE2													0.08	0.04	0.05	0.05	0.03	0.02	0.01	0.01	0.01	0.03	0.00	0.01
	SE3														0.07	0.05	0.00	0.04	0.02	0.05	0.02	0.02	0.06	0.02	0.00
	SE4															0.02	0.00	0.01	0.02	0.05	0.02	0.05	0.03	0.02	0.02
	FIs																0.03	0.05	0.03	0.02	-0.03	0.03	0.01	-0.01	-0.02
	FIn																	0.04	0.00	0.00	0.00	-0.01	0.00	-0.01	0.00
	EE																		0.05	0.05	0.00	0.01	0.04	0.01	0.00
	LV																			0.15	0.00	0.02	0.00	-0.01	-0.01
	LT																				-0.03	0.02	0.03	-0.01	0.02
	NO3																					0.02	0.01	0.02	0.01
	NO4																						0.02	-0.01	0.00
	NO1																							0.01	0.01
	NO2																								0.04
	NO5																								

The correlations are presented only for the hour ahead forecast errors (for 5 minute resolution) using the adjustment algorithm. The presented values are calculated using all the five years of simulated data.